Interlocking Folded Plate - Integral Mechanical Attachment for Structural Wood Panels

Christopher Robeller [*1] and Yves Weinand [†1]

[1]Timber Construction Laboratory IBOIS, EPFL

June 20, 2015

Abstract

Automatic joinery has become a common technique for the jointing of beams in timber framing and roofing. It has revived traditional, integral joints such as mortise and tenon connections. Similarly, but only recently, the automatic fabrication of traditional cabinetmaking joints has been introduced for the assembly of timber panel shell structures. First prototypes have used such integrated joints for the alignment and assembly of components, while additional adhesive bonding was used for the load-bearing connection. However, glued joints cannot be assembled on site, which results in several design constraints.

In this paper, we propose the use of dovetail joints without adhesive bonding, on the case study of a timber folded plate structure. Through their single-degree-of-freedom (1DOF) geometry, these joints block the relative movement of two parts in all but one direction. This presents the opportunity for an interlocking connection of plates, as well as a challenge for the assembly of folded plate shells, where multiple non-parallel edges per plate must be jointed simultaneously.

1 Introduction

Architectural designs have often been inspired by folded shapes such as Origami, however the folding principle can rarely be applied to building structures directly. Instead, many folded plates have been cast as concrete thin-shells in the 1960s. These constructions were labour-intensive and required elaborate formwork for the in-situ casting.

Prefabricated constructions with discrete elements made from fiber-reinforced plastics have been researched in the 1960s. [1]

Folded plates built from laminated timber panels have been presented by C. Schineis [19] (Glulam) and H. Buri [2] (Cross-laminated Timber). These designs combine the elegant and efficient shape of folded plate shells with the advantages of structural timber panels, such as CO2 storage and a favorable weight-to-strength ratio. However, a major challenge in the design of a timber folded plate is presented by the joints: Since timber panels cannot be folded, a large amount of edgewise joints has to provide two main functions. One of these functions is the load-bearing behaviour, where *connector features* of the joints must provide a sufficient stiffness and rigidity. The second main function of the joints is the assembly of the parts, where *locator features* of the joints are essential for a precise and fast positioning and alignment of the parts.

B. Hahn [5] examined the structural behaviour of a first timber folded plate shell which was built from plywood and assembled with screwed miter joints, concluding that the load-bearing performance could be improved significantly with more resistant connections.

Inspiration for such improvements may be found in *integral mechanical attachment* techniques, the oldest known technique for the jointing of parts, where the geometry of the parts themselves blocks their relative movements [13]. Such integrated joints have recently been re-discovered by the timber construction industry. Beginning in 1985, mortise-and tenon joints have been repatriated in timberframe and roof constructions [7]. Only very recently, integrated joints have also been proposed for the edgewise jointing of timber panels. In the ICD/ITKE Reserach Pavilions 2011 [12] and

2013 [11], fingerjoints have been applied to plywood panels and an application of dovetail joints for cross-laminated timber panels (CLT) was presented in the IBOIS Curved Folded Wood Pavilion 2013 [18]. In these prototype structures, the integrated joints have played an important role for the assembly of the components. They have also participated in the load-bearing connection of the parts, but additional adhesive bonding was needed. With few exceptions [6], such glued joints cannot be assembled on site, because they require a curing period with a specific constant temperature and humidity [15]. Therefore, their application is limited to off-site assembly of larger components, which complicates both transport and handling while still requiring additional connectors for the final assembly.

In this paper, we propose the use of dovetail joints without additional adhesive bonding, on the case study of a timber folded plate shell. (Figure 1).

Through their single-degree-of-freedom (1DOF) geometry, these joints block the relative movement of two parts in all but one direction. This presents the opportunity for an interlocking connection of plates, as well as a challenge for the assembly of folded plate shells, where multiple non-parallel edges per plate must be jointed simultaneously.

1.1 Dovetail joint geometry and mechanical performance

Using polygon mesh processing, we describe an edgewise joint based on its edge E. From the mesh connectivity, we obtain the edge vertices p and q and the adjacent faces F_0 and F_1 with their face normals n_0, n_1. We use the polygon mesh to represent the mid-layer of timber panels with a thickness t and offset F_1 and F_2 at $\pm\frac{t}{2}$ to obtain the lines L (Figure 2a). From a division of E, we obtain the points X_j for a set of reference frames $\{u_1, u_2, u_3\}$, where $u_1 \parallel \vec{pq}$ and $u_2 \parallel n_0$ (Figure 2b). A finger joint geometry is obtained from an intersection of planes located at X_j, normal to u_1, with the four lines L.

Without additional connectors, finger joints are a kinematic pair with three degrees of freedom (3DOF), also called *planar joints*. They can resist shear forces parallel to the edge and in-plane compressive forces. However depending on the plate geometry, thickness and most of all rotational stiffness of the connection detail, bending moments are also transferred between the plates. Also, due to the rotation of the plate edge caused by bending, in-plane traction forces perpendicular to the edge line appear and their magnitude increases under asymmetrical loads. Such forces, which occur as a result of out-of-plane loading, cannot be supported only by shear and in-plane compression resistant joints.

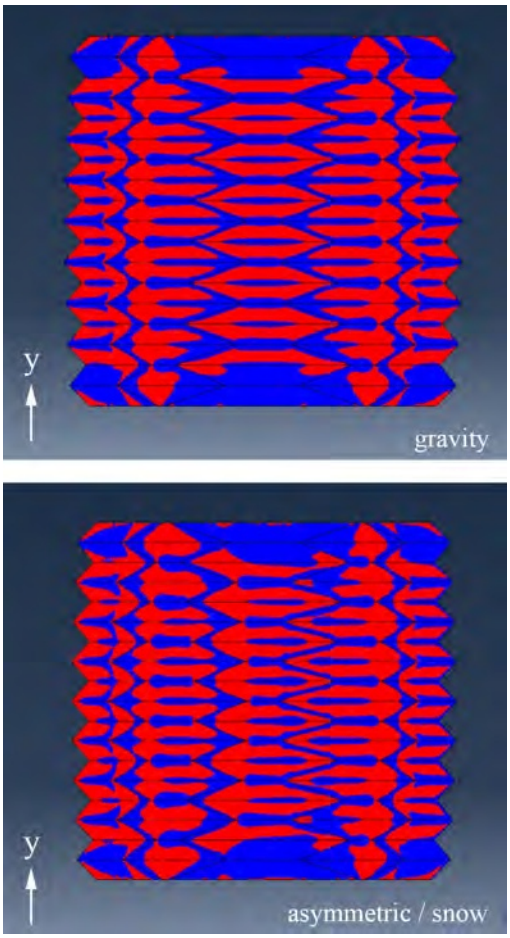

Figure 3: FEM analysis (top view) of a 3x3m, 21mm Kerto-Q folded plate thin shell assuming fully stiff joints. Distribution of traction (red) and compression (blue) stresses in the y direction. Top: gravity load case. Bottom: asymmetric snow load.

On a dovetail joint (Figure 2d,e), the intersection planes on the points X_j are normal to a rotated vector w_1. It is obtained from a rotation of the reference frame $\{u_1, u_2, u_3\}$ about u_3 at an alternating angle $\pm\theta_3$. The resulting rotated side faces reduce the dovetail joints degrees of freedom to one translation $\vec{w_3}$ (1DOF). Simek and Sebera [20] have suggested $\theta_3 = 15°$ for spruce plywood panels. Such prismatic joints can only be assembled or disassembled along one assembly direction $\vec{v} = \vec{w_3}$. In addition to the finger joints resistance to shear and compressive forces, dovetail joints can, without adhesive bonding, also resist bending moments and traction forces which are not

Figure 1: Folded thin shell prototype built from 21mm LVL panels, assembled with single-degree-of-freedom dovetail joints without adhesive bonding. Components interlock with one another

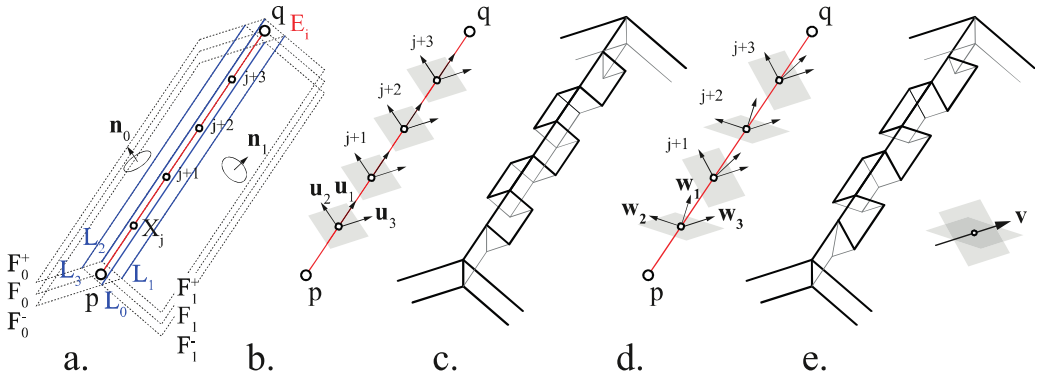

Figure 2: Joint geometry. a: Basic parameters, b: Intersection planes (grey) normal to $\vec{pq}$, c: 3DOF joint, d: Rotated intersection planes (grey) normal to $\vec{w_j}$, e: 1DOF joint

parallel to $\vec{v}$. Due to the inclination of the side faces of the joint, resistance to these forces can be improved significantly. In that way the inclined faces take over the role that the glue would have in a finger joint. (Figure4)

1.2 Fabrication Constraints

One of the main reasons for the resurgence of finger and dovetail joints is the possibility of automatic fabrication. However, the mechanical performance of the joints depends on fabrication precision. At the same time, fast machine feed rates are important for a time-efficient production. We have fabricated such joints with a robot router and a gantry router, achieving higher precision with the gantry machine, which is more stiff and provides a higher repeat accuracy.

The variability of the machine-fabricated joints is enabled by the 5-axis capability of modern routers: Although traditional edgewise joints in cabinetmaking were used for orthogonal assemblies, both the finger and dovetail joint can also be applied for non-orthogonal fold angles, which was essential for the reference projects mentioned before. However, there are certain fabrication-related constraints for machine-fabricated dovetail joints. In order to integrate the joint fabrication directly with the panel formatting, we use a side-cutting technique [8], which is limited to a tool inclination β_{max}. We obtain this limit from the specific geometry of the tool, tool-holder and spindle used for the joint fabrication. (Figure 5)

The parts can be assembled in two ways, as shown in figure 5, which allows to address a larger range of dihedral angles φ. From this we obtain the fabrication-constrained most acute fold $\varphi_{min} = 90° - \beta_{max}$ and most obtuse fold $\varphi_{max} = 90° + \beta_{max}$. With standard cutting tools, this technique allows for the jointing of acute folds up to

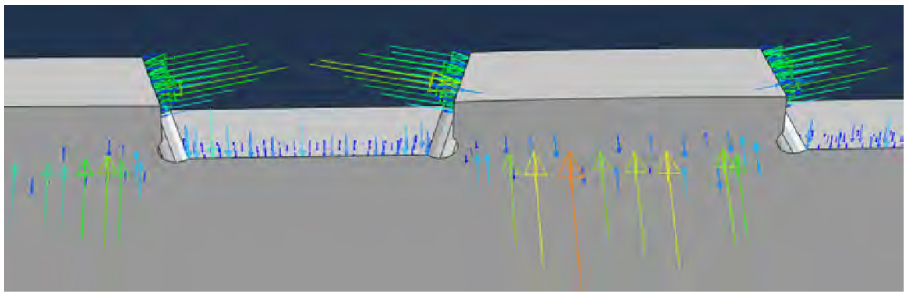

Figure 4: FEM simulation of bending on a dovetail joint connecting two Kerto-Q 21mm LVL panels. The bending moment applied is transformed into compression, normal and shear forces parallel to the inclined contact faces.

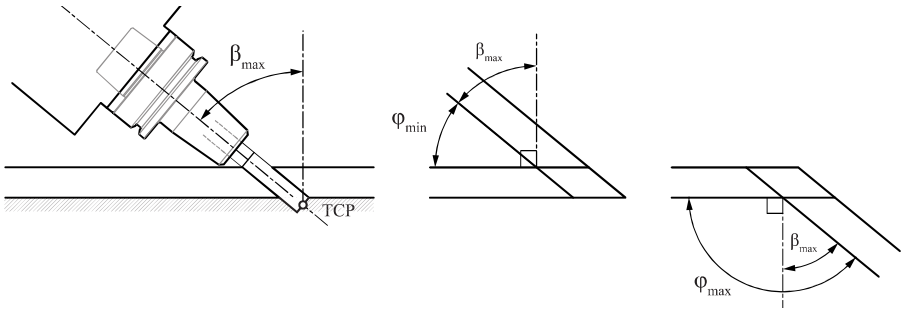

Figure 5: Fabrication Constraints. Side-cutting technique used for the automated fabrication of 1DOF edgewise joints with common 5-axis CNC routers. The maximum tool inclination β_{max} results from the tool and the tool holder geometry. From this we obtain the range of possible *dihedral angles* $\pm\varphi$ between panels.

$\varphi = 50°$, which is ideal for folded plate structures. Very obtuse fold angles $\varphi \geq 140°$, which might be required for smooth segmented plate shells, cannot be fabricated with this method.

1.3 Simultaneous Assembly of Multiple Edges

The assembly of doubly-corrugated folded plates requires the *simultaneous* joining of multiple edges per component (Figure 1), which has implications on both the shell and the joint geometry.

For multiple 1DOF-jointed edges, simultaneous assembly is only possible if the individual assembly directions $\vec{v}$ are parallel. With a normal dovetail joint geometry (Figure 7a), this is not the case: A simultaneous assembly is only possible for parallel edges, which allows only for rectangular assemblies, such as drawers or a cabinets.

In order to simultaneously join non-parallel edges, we must rotate the assembly direction v of the joints to make them parallel. This possibility is known from Japanese cabinetmaking [9], where certain joints, like the Nejiri Arigata Joint (Figure 7b), are assembled diagonally, along a vector that does not lie on either one of the two planes. While European dovetail form a prism with a single tab,

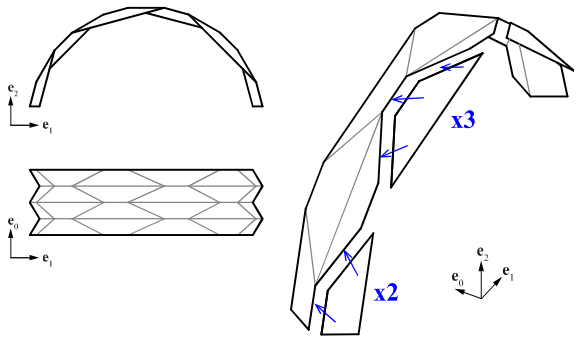

Figure 6: The assembly of a folded plate from discrete elements (left side) requires the *simultaneous* assembly of non-parallel edges. (right side) We rotate the insertion direction of our 1DOF joints, to make the insertion vectors of simultaneously jointed edges parallel. We chose a hexagon reverse fold pattern which requires only moderate rotations.

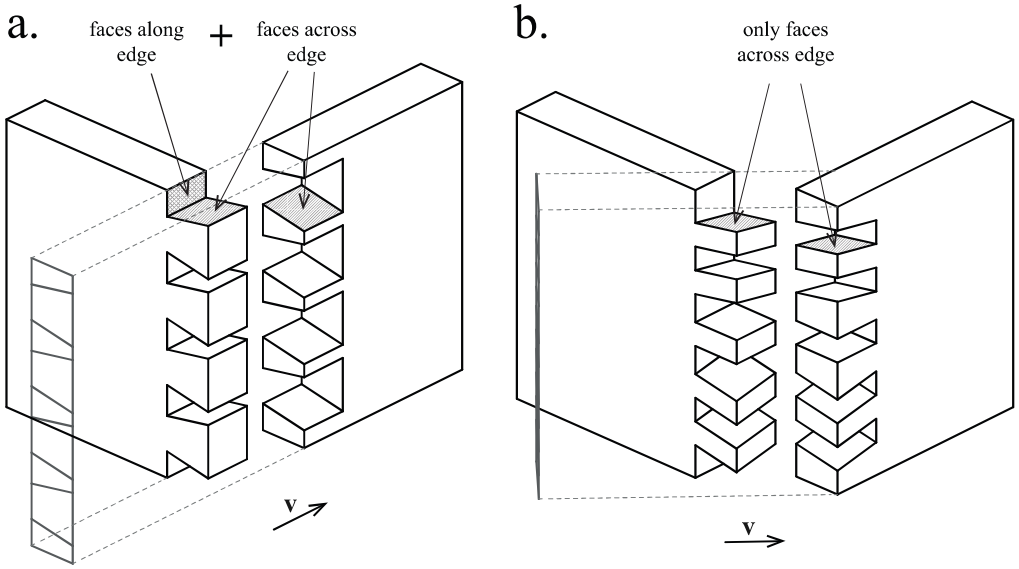

Figure 7: a. Dovetail Joint, b. Nejiri Arigata Joint

using faces both acrioss and along the edge, the Nejiri Arigata joints form a prism using multiple, differently shaped tabs.

We extend this Japanese technique to a *vector subset* of possible assembly directions. Figure 8 shows that the rotation about the edge line is constrained to $180° - \varphi_i$. The vector subset is large for acute and small for obtuse fold angles. This is particularly important when joining multiple edges simultaneously, because an intersection must be found between multiple vector subsets (Fig. 9). If there is an intersection, the parts can be joined simultaneously along any direction within the intersection of the subsets.

Finally we extend this concept to a 3-dimensional rotation (Fig. 10). This is possible through a second rotation θ_2, which is constrained to a maximum value of $\pm\theta_{2,max}$. The limitation results from multiple other corelated parameters, such as θ_1 and β_{max}. We call the resulting 3D vector subset *rotation window*.

With this method, we can search for a joining solution for the prototype in figure 6. We compute rotation windows S_1, S_2, S_3 for the edges E_1, E_2, E_3 and overlay them at their center point. Figure 11 shows that there is a common vector subset $S_1 \bigcap S_2 \bigcap S_3$ between these three edges, we can choose our assembly direction within it.

As a result of these limited rotations, the angle between neighbouring, simultaneously joined edges cannot be very acute. Folded plate patterns like the Herringbone, the Diamond, or the Hexagon pattern, which we chose for our prototypes, (Figure 6) work well for our joining tech-

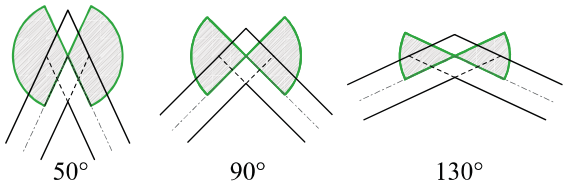

Figure 8: 2D vector subset

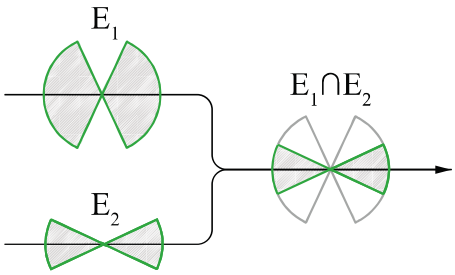

Figure 9: 2D simultaneous assembly

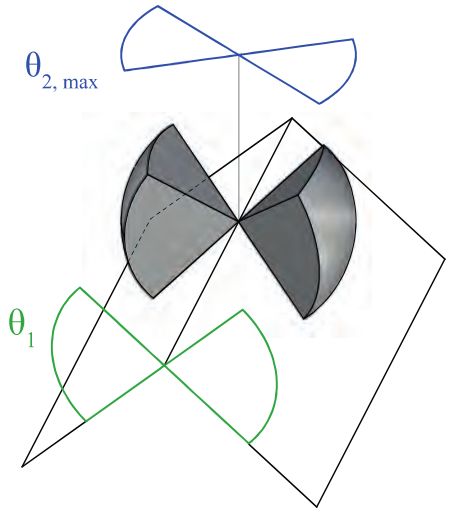

Figure 10: 3D vector subset

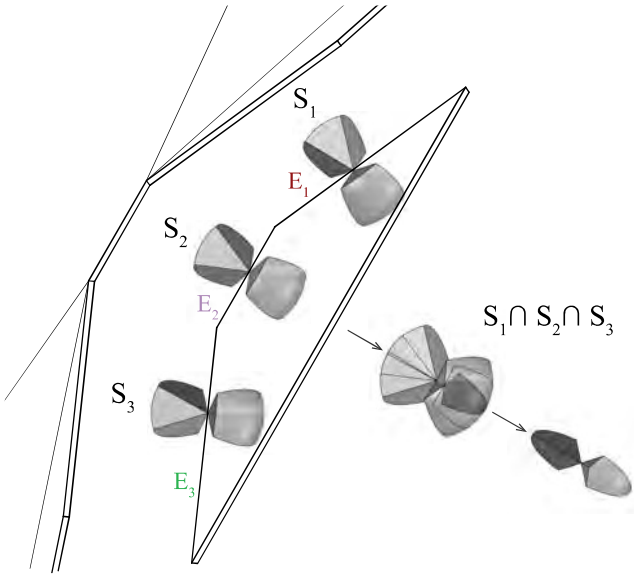

Figure 11: 3D simultaneous assembly

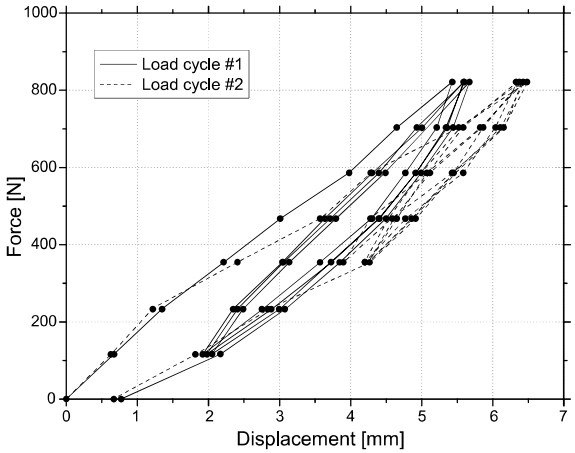

Figure 13: Series of 3-point flexural tests on the small scale interlocking arch prototype built from Metsawood 12mm birch plywood panels.

nique. Another essential feature provided by these reverse-folds are the acute fold angles, which easily satisfies the fabrication-constrained range of $\varphi_{min} = 50°$ to $\varphi_{max} = 140°$.

2 Interlocking Arch Prototype

In an assembly of multiple components (Figure 12), a step-by-step sequence must be planned for the assembly of the parts. The completed structure can only be disassembled piecewise in the reverse order of assembly. In this way, the elements interlock with one another like a *Burr Puzzle* [22].

Each joint consists of two parts, which must be parallel during assembly. We therefore chose a folded plate geometry with relatively short edges. The manual assembly of long edges may be more difficult but can be simplified with a modified joint geometry. It is important to know the approximate direction of insertion for each part, as this is not easily visible through the joint geometry. Deformations of the arch during the assembly should be minimised. We have assembled this first prototype lying on the side. However larger assembly may require temporary punctual supports. Although the in-plane dimensional stability of the Kerto-Q panels is very high, panels may be slightly warped and some force may be necessary during assembly. While we have simply used a rubber hammer, more advanced techniques could be applied.

To understand the mechanical behaviour of the built prototype, we have applied a vertical load at mid-span of the arch and measured the vertical deflection at the same point. The total load of 821N was applied in two identical load cycles consisting of four loading/unloading sub-cycles. First, a vertical load of 117N was applied in seven steps, after which the load of the last four steps was removed. The loading and unloading of the last four steps was repeated three more times, after which the complete load was removed and the residual deflection was measured. (Figure 13)

Under a vertical load equal to the archs dead weight of 9.8kg (98N), the deflection measured at mid-span was 2mm. From this we obtain a span-to-deflection-ratio of $L/750$ and the arch's structural efficiency which reaches 8.6 when loaded with 821N (ratio of the maximal load over the dead weight of the arch).

3 Interlocking Shell Prototype

3.1 Automatic Geometry Processing

Using the RhinoPython application programming interface, we have developed a computational tool which lets us instantly generate both the geometry of the individual components and the machine G-Code required for fabrication. The tool processes arbitrary polygon meshes, and generates 1DOF joints for all non-naked edges where the fold angle φ is larger than φ_{min} and smaller than φ_{max} shown in figure 5 (non-smooth meshes). It also requires an input of edge identifier tuples identifying those edges which must be jointed simultaneously, as well as the thickness of the LVL panels. Exploiting this geometrical freedom, we have tested our computational tool on the design of a folded plate shell prototype with an alter-

Figure 12: Folded-plate arch prototype built from 12mm birch plywood (9-layer, I-I-I-I-I). Assembled without adhesive bonding or metal fasteners. Span 1.65m, self-weight 9.8kg.

nating convex-concave transversal curvature. The shell spans over 3m at a thickness of 21mm, using Kerto-Q structural grade LVL panels (7-layer, I-III-I). (Figure 14)

Comparing this doubly-curved folded plate with a straight extrusion (as tested by H. Buri [2]), it can be concluded that the slight double-curvature proves to be very beneficial when it comes to global deflections, for example those caused by wind loads. Deflections for the doubly-curved shell geometry in the vertical direction are up to 39% smaller and up to 13% smaller in the lateral direction than the ones for the straight extrusion one.

3.2 Assembly

Due to the different assembly directions of its 239 joints, the 107 components components in our prototype interlock with one another, similar to a *Burr Puzzle* [22]. Figure 15 shows a part of a so called *non-directional blocking graph* (NDBG), which was inroduced by Wilson and Latombe [21].

In such a graph, single arrows indicate that parts can be removed from the assembly. Two opposite arrows between parts indicate that the connection is blocked. In order to remove blocked parts, the blocking parts must be removed first. Our graph illustrates a left-to-right assembly. On the right side, part number 86 is being inserted. It connects to three other plates and blocks all other parts in the graph. In such a configuration, the final part remains removable, it is called the *key*.

Figure 16 shows the parts from figure 15 in 3D, demonstrating how the component based on mesh face F_{86} is being inserted. Its three edgewise joints E_{41}, E_{68} and E_{89} must be assembled simultaneously. The three assembly vectors of the edges $\vec{v_{41}}$, $\vec{v_{68}}$ and $\vec{v_{89}}$ have been rotated to be parallel. The same applies for the adjacent edges on the left side of the faces F_{67}, F_{69}, F_{88}, F_{103} and F_{105} (see figure 15). Within the rotation window of the edge, we can freely rotate $\vec{v}$ for these edges (the greater the angle between $\vec{v}$ and the main direction of traction e_1, the better).

3.3 Completed Shell Prototype and Load Test

Figure 17 shows the completed folded plate prototype, with a span of 3m and a shell thickness of 21mm. Boundary conditions that restrain displacements of the supports in every direction, but allow rotations, were applied on both sides. A longitudinal line load was introduced along the top of the shell and vertical displacement was measured at center point. (Figure 18)

The prototype structure was also modelled in

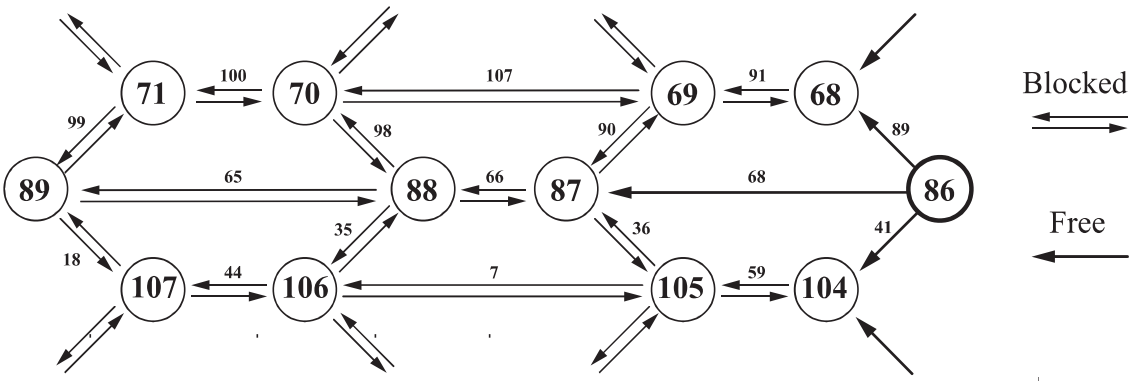

Figure 15: Partial connectivity, assembly and blocking graph of the folded plate shell prototype. (Left-to-right assembly) Large numbers represent mesh faces, small numbers represent mesh edges.

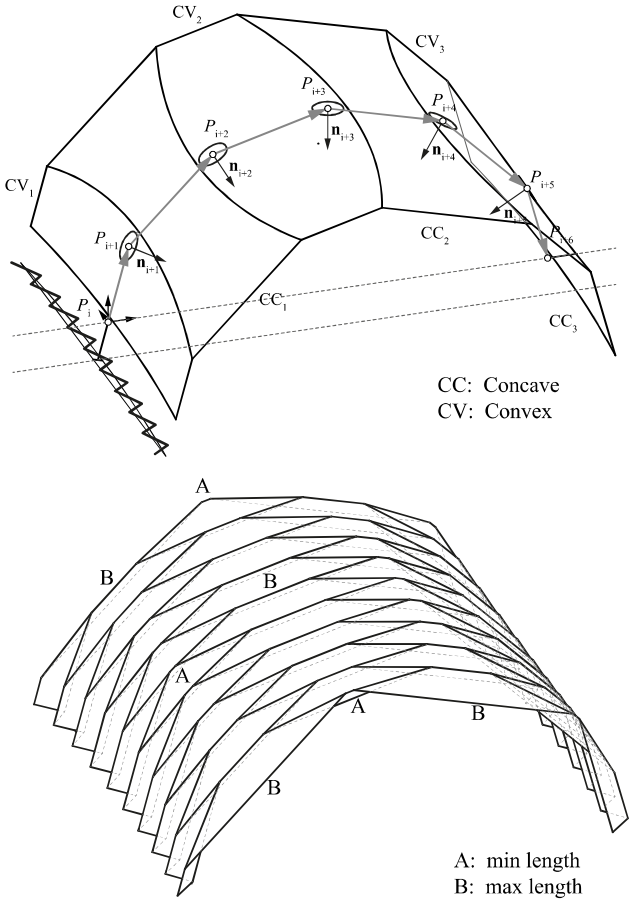

Figure 14: Doubly-curved folded-plate: The radius ($R = 17m$) of the transversal curvature is determined by the folded plates maximum amplitude h [2], which is inversely proportional to the number of segments m of the cross-section polyline (grey). We obtain this polyline from a circular arc divided into segments of equal length. The interior angle $\gamma = ((m-2)*180)-m$ of this polyline is proportional to all fold angles φ. The geometry of our prototype was fabrication-constrained to a maximum component length $B \leq 2.5m$

FE analysis software (Abaqus) and loaded in the same way. The plates were modelled using shell elements, where the mid-surface is used to represent the 3D plate and transverse shearing strains are neglected. Connections between the plates were considered as completely rigid in order to obtain minimal displacements of the structure. By comparing the displacements of the structure with infinitely stiff joints with the ones measured on the prototype, we obtained information about the actual semi-rigidity of the joints. The results obtained from the testing of the large scale prototype showed that the load of 25kN, that corresponds to the proportional limit of the load-displacement curve, causes a vertical displacement of 23mm. In the FE model, the load applied in the same manner caused a vertical displacement of 2.6mm.

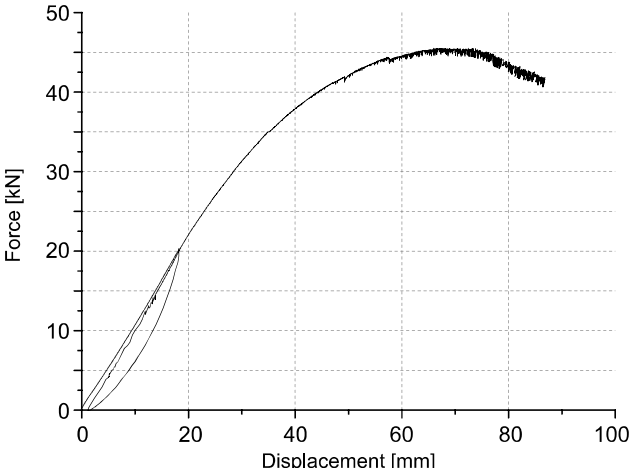

Figure 18: Load-displacement curve of the shell prototype. A longitudinal line load was introduced along the top of the shell. Vertical displacement was measured at the center point.

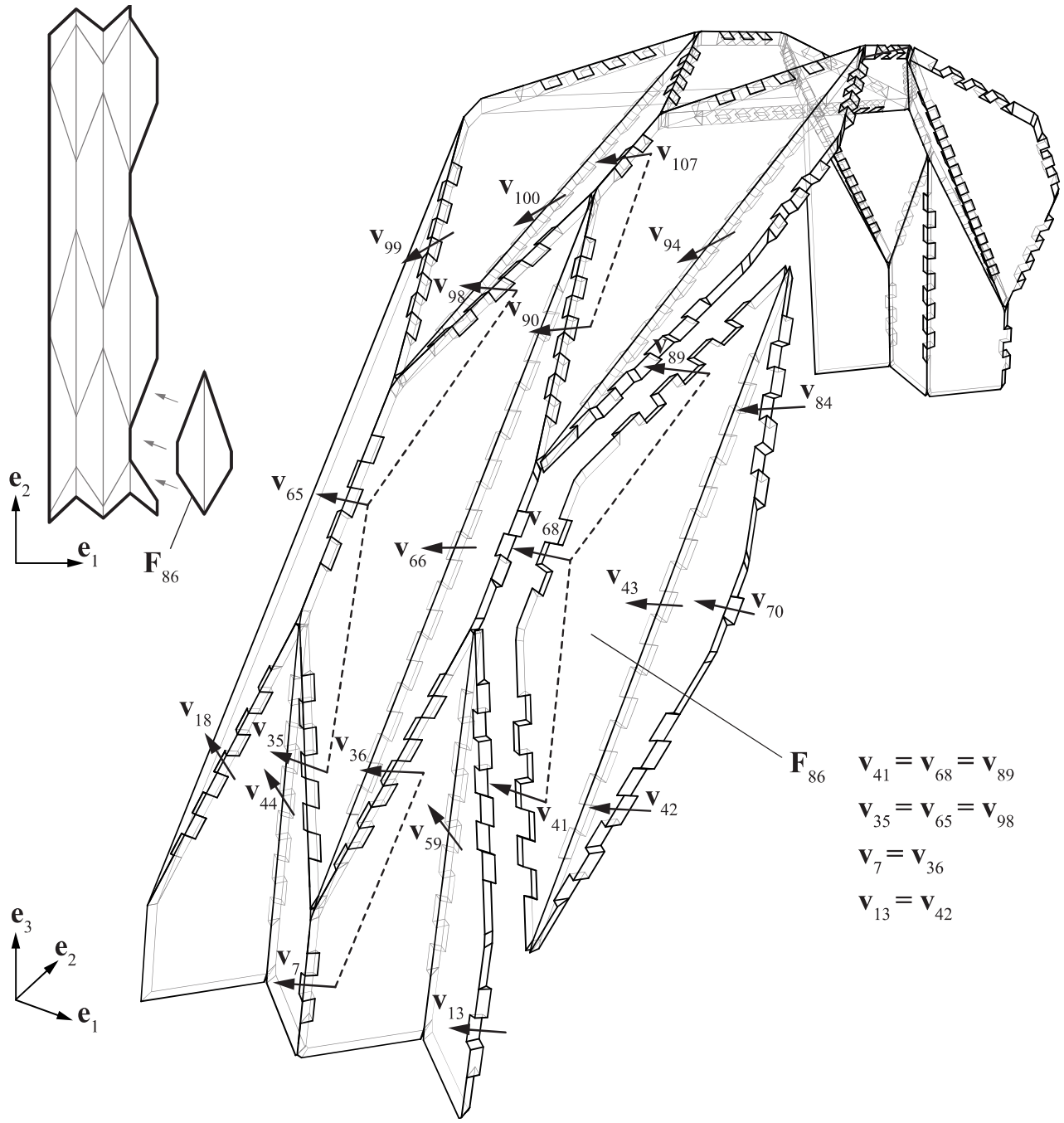

Figure 16: Left-to-right assembly of the Interlocking folded plate shell prototype. Built from Kerto-Q structural grade LVL panels (7-layer, I-III-I))

Figure 17: Folded-plate shell prototype, built from 21mm LVL panels. With a self-weight of 192kg, the prototype with a span of 3m was tested with a line-load up to 45kN.

4 Conclusion

A timber folded plate shell combines the structural advantages of timber panels with the efficiency of folded plates. However, in such discrete element assemblies, a large amount of semi-rigid joints must provide sufficient support for the adjacent plates in oder to ensure an efficient load-bearing system. This remains a challenge with much potential for improvements [5].

Integrated edgewise joints present an interesting addition and an alternative to state-of-the-art connectors: Compared to adhesive bonding, such joints can be assembled rapidly on site. Also, compared to costly metal plates and fasteners, which are typically required in large quantities [14], the fabrication of integrated joints is not more expensive. The replacement or reduction of metal fasteners with an integrated mono-material connection includes advantages such as improved aesthetics, ease-of recycling or a homogenous thermal conductivity of the parts, which can reduce condensation and decay. [4] Another particular advantage is the possibility to join thin panels: The current technical approval for the Kerto-Q panels does not permit screwed joints on panels with a thickness of less than 60mm. [3]

Recent experimental projects, which we introduced in chapter 1, have already demonstrated first applications of integrated edgewise joints for timber panels. This paper followed up on these projects, examining the particular advantages, potential and challenges of 1DOF joints for timber folded plate shells. We have demonstrated how this joint geometry helps resisting the forces which occur in such structures. In addition to the load-bearing connector features, the joints provide locator features, which allow for precise positioning and alignment of the parts through the joint geometry. This improves both accuracy and ease of assembly. Furthermore, we have presented a solution for the simultaneous assembly of multiple edges per panel, which is essential for the application of 1DOF joints in a folded plate shell structure. The per edge "rotation window" introduced in section 1.3 integrates the joint constraints related to assembly and fabrication. It can be processed algorithmically and gives instant feedback on whether or not a set of non-parallel edges can be jointed simultaneously. This provides a tool for the exploration of a variety of alternative folded plate shell geometries.

The prototypes presented in this paper already suggest possible patterns and demonstrate the reciprocal relationship between the geometry of the plates and the joints. Two built structures allowed us to test and verify the proposed methods for fabrication and assembly while providing valuable information about the load-bearing capacity of the integrated joints.

For the application in a large-scale building structure, further research is required to determine if the integrated joints can replace additional connectors entirely or reduce their amount. A possible combination of integrated joints with additional metal fasteners has been demonstrated recently in the LaGa Exhibition Hall [10]. Another possibility would be a combination of the 1DOF joints with integrated elastic interlocks. [17]

Acknowledgments

We would like to thank Andrea Stitic and Paul Mayencourt for their support with the finite element models and load testing of the prototypes, as well as Gabriel Tschanz and Francois Perrin for assisting with the fabrication and assembly of prototypes. We also thank Jouni Hakkarainen and the Metsa Group for the supply of information and materials.

References

[1] B.S. Benjamin and Z.S. Makowski. The analysis of folded-plate structures in plastics. In *Proceedings of a conference held in London*, pages 149–163. Pergamon Press, London, 1965.

[2] Hani Buri and Yves Weinand. BSP Visionen - Faltwerkkonstruktionen aus BSP-Elementen. In *Grazer Holzbau-Fachtage*, 2006.

[3] DIBt. *Allgemeine bauaufsichtliche Zulassung Kerto-Q Z-9.1-100, Paragraph 4.2 and Attachment No 7, Table 5.* Deutsches Institut für Bautechnik, 2011.

[4] Wolfram Graubner. *Holzverbindungen, Gegenüberstellung von Holzverbindungen Holz in Holz und mit Metallteilen.* Deutsche Verlags-Anstalt Stuttgart, 1986.

[5] Benjamin Hahn. Analyse und beschreibung eines räumlichen tragwerks aus massivholzplatten. Master's thesis, EPFL, Lausanne, 2009. Master Thesis.

[6] HESS. Hess limitless, 2014. http://www.hess-timber.com/de/produkte/.

[7] Hundegger. Hans Hundegger Maschinenbau GmbH, Hawangen, Germany, 2014. http://www.hundegger.de/en/machine-building/company/our-history.html.

[8] Peter Koch. *Wood Machining Processes.* Wood Processing. Carl Hanser Verlag GmbH & Co. KG, 1964.

[9] Tetsuya Kōndo. *Dento kanehozo kumitsugi : Sekkei to seisaku no jissai.* LLP Gijutsushi Shuppankai, Tokyo : Seiunsha, 2007.

[10] Oliver Krieg, Tobias Schwinn, Achim Menges, Jian-Min Li, Jan Knippers, Annette Schmitt, and Volker Schwieger. Computational integration of robotic fabrication, architectural geometry and structural design for biomimetic lightweight timber plate shells. In *Advances in Architectural Geometry 2014.* Springer Verlag, 2014.

[11] Oliver David Krieg, Zachary Christian, David Correa, Achim Menges, Steffen Reichert, Katja Rinderspacher, and Tobias Schwinn. Hygroskin: Meteorosensitive pavilion. In *Fabricate 2014 Conference Zurich*, pages 272–279, 2014.

[12] Riccardo la Magna et al. From nature to fabrication: Biomimetic design principles for the production of complex spatial structures. *International Journal of Spatial Structures*, Vol. 28 No. 1:27–39, 2013.

[13] Robert W. Messler. *Integral Mechanical Attachment: A Resurgence of the Oldest Method of Joining.* Butterworth Heinemann, 2006.

[14] Helmuth Neuhaus. *DIN EN 1995 (Eurocode 5) - Design of timber structures.* DIN Deutsches Institut fur Normung e. V., 2004.

[15] Purbond. *National Technical Approval Z-9.1-711 / Single-component polyurethane adhesive for the manufacture of engineered wood products.* Deutsches Institut für Bautechnik, 2011.

[16] Christopher Robeller. *Integral Mechanical Attachment for Timber Folded Plate Structures.* PhD thesis, ENAC, Lausanne, 2015.

[17] Christopher Robeller, Paul Mayencourt, and Yves Weinand. Snap-fit joints: Integrated mechanical attachment of structural timber panels. In *Proceedings of the 34th International Conference of the Association of Computer-aided Design in Architecture ACADIA, Los Angeles, USA*. Riverside Architectural Press, 2014.

[18] Christopher Robeller, SeyedSina Nabaei, and Yves Weinand. Design and fabrication of robot-manufactured joints for a curved-folded thin-shell structure made from clt. In Wes McGee and Monica Ponce de Leon, editors, *Robotic Fabrication in Architecture, Art and Design 2014*, pages 67–81. Springer International Publishing, 2014.

[19] Regina Schineis. Gefalteter Klangkoerper Musikprobensaal Thannhausen / Thannhausen Rehearsal Room. In *10. Internationales Holzbau Forum (IHF), Garmisch-Partenkirchen*, 2004.

[20] Vaclav Sebera and Milan Simek. Finite element analysis of dovetail joint made with the use of cnc technology. *Acta Universitatis Agriculturae Et Silviculturae Mendelianae Brunensis*, Volume LVIII:321–328, 2010.

[21] Randall H. Wilson and Jean-Claude Latombe. Geometric reasoning about mechanical assembly. *Artificial Intelligence*, 71(2):371 – 396, 1994.

[22] Edwin Wyatt. *Puzzles in Wood*. Bruce Publishing Co., 1928.